Available online at www.sciencedirect.com
SCIENCE DIRECT®
Diamond and Related Materials 13 (2004) 1171–1176
DIAMOND AND RELATED MATERIALS
www.elsevier.com/locate/diamond

Low-temperature plasma enhanced chemical vapour deposition of carbon nanotubes

S. Hofmann*, B. Kleinsorge, C. Ducati[1], A.C. Ferrari, J. Robertson

Engineering Department, University of Cambridge, Trumpington Street, Cambridge CB2 1PZ, UK

Abstract

Vertically aligned carbon nanotubes were selectively grown at temperatures as low as 120 °C by plasma enhanced chemical vapour deposition. We investigated the effects of acetylene, ethylene and methane as carbon source gases together with ammonia as an etchant and nickel as catalyst material. The diluted acetylene plasma gave the highest nanotube growth rate and showed the most intense C_2 Swan bands in optical emission. The activation energy for the growth rate was found to be 0.23 eV, much less than for thermal chemical vapour deposition (1.2–1.5 eV). This suggests growth occurs by surface diffusion of carbon on nickel. The result allows more cost-effective nanotube production, direct growth of nanotubes onto low-temperature substrates like plastics, and could facilitate carbon nanotube integration into sensitive nanoelectronic devices.

Keywords: Carbon nanotubes; Plasma CVD; Catalytic processes; Nanotechnology

1. Introduction

Based on their unique properties, carbon nanotubes (CNTs) and less crystalline carbon nanofibres (CNFs) provide ideal model systems to access low dimensional physics and could play a key role in future nanotechnology. Numerous methods to grow CNTs have been developed, including arc-discharge, laser ablation and chemical vapour deposition [1–3]. However, only a few methods allow the controlled growth of nanotubes directly on a substrate, which is important for many applications, as the individual manipulation of CNTs is difficult and expensive due to their size. Selective, aligned growth of CNTs on silicon and glass substrates has been demonstrated by plasma enhanced chemical vapour deposition (PECVD) [4,5]. Despite the high level of growth control, PECVD of CNTs typically involves temperatures over 500 °C, which limits the choice of substrate materials and integration processes. Growth at lower temperatures has been reported [6], using, however, large grain sized Ni catalyst powder, which shows poor substrate adhesion and does not allow patterning or alignment of the as-grown CNFs.

This paper reports the selective growth of vertically aligned nanofibres at temperatures as low as 120 °C on prepatterned substrates using a dc PECVD system [7]. We investigate the effects of acetylene, ethylene and methane as carbon source gases, together with ammonia as an etchant and nickel as catalyst material. Focussing on acetylene, a systematic study of the temperature dependence of the CNF growth rate has been carried out. The activation energy for low-temperature PECVD is compared to the activation energies of carbon diffusion in nickel and a growth model is discussed.

2. Experimental details

The aligned CNFs were grown using a dc PECVD system in a stainless steel diffusion pumped vacuum chamber with a base pressure below 10^{-6} mbar. The polished n-type Si(100) substrates were covered with a 20-nm thick SiO_2 layer, grown by thermal oxidation or low-temperature electron cyclotron resonance. The SiO_2 acts as a diffusion barrier between the catalyst material and the Si substrate preventing the formation of a silicide. At low substrate temperatures the deposition of a separate diffusion barrier might be omitted, however, in this comparative growth study we always used a SiO_2 layer to exclude substrate effects. A 6-nm-thick Ni film was deposited onto the oxide by magnetron

*Corresponding author. Tel.: +44-1223-764093.
E-mail address: sh315@cam.ac.uk (S. Hofmann).
[1] *Present address* Department of Materials Science and Metallurgy, University of Cambridge, Cambridge CB2 3QZ, UK.

0925-9635/04/$ - see front matter © 2003 Elsevier B.V. All rights reserved.
doi:10.1016/j.diamond.2003.11.046

sputtering. The catalyst was patterned either by shadow masks for 10 μm feature sizes or by e-beam lithography using poly-(methylmethacrylate) as photoresist for 100 nm feature sizes.

The growth procedure is reported in detail elsewhere [7]. Briefly, the samples were heated up for 15 min in ammonia to reach the desired temperature. A dc discharge was ignited by applying a fixed voltage of 600 V between the graphite heater stage and the gas shower head (anode, 2 cm above stage). The carbon source gas was introduced via a separate mass flow controller at a fixed flow ratio. A stable discharge current of typically 30 mA was maintained for deposition times of 10 min to 1 h. The temperature was measured with a thermocouple mounted on a Si substrate of equivalent original sample thickness. It has to be emphasised, that as the set-up is optimised for high throughput, the thermal contact between sample and heater stage is poor and, therefore, the temperature measured for CNF growth on top of the substrate can be significantly lower compared to values measured directly on the heater stage. Temperature labels were used as additional calibration standards at low temperatures. For resistive heating above 120 °C, no increase in bulk substrate temperature due to the plasma could be measured.

The plasma was analysed by optical emission spectroscopy (OES, Verity Instruments EP200Msd). The OES spectra were taken with a glass fibre cable positioned inside the vacuum chamber at a distance of 5 cm from the plasma discharge. The dimensions and structure of the as-grown CNFs were analysed by scanning electron microscopy (SEM, Jeol 6340 FEGSEM), high-resolution transmission electron microscopy (HREM, Jeol JEM 4000EX, 400 kV) and Raman spectroscopy (Renishaw MicroRaman 1000, 514.5 nm Ar-ion laser). For HREM analysis the CNFs were removed from the substrate and dispersed onto Cu TEM grids or lacey carbon grids.

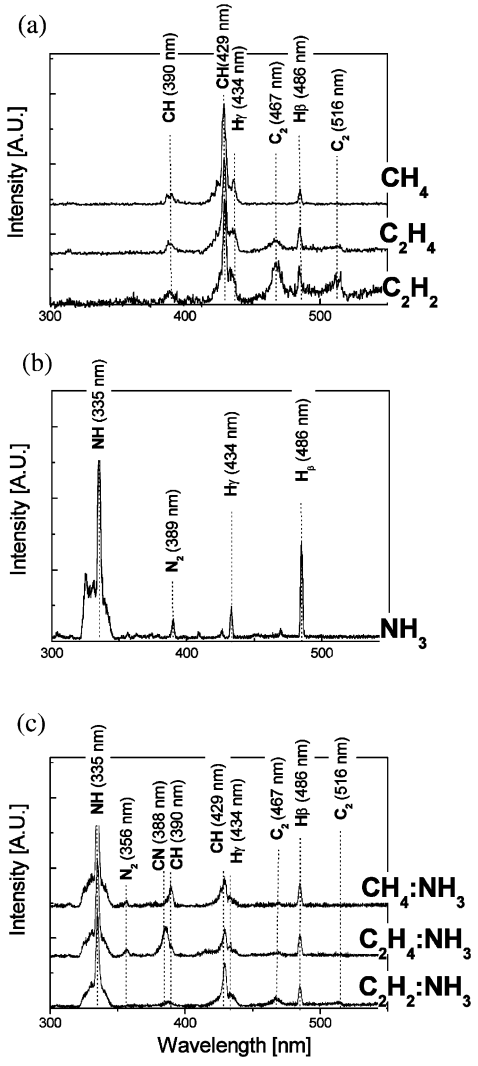

Fig. 1. Optical emission spectra of a 600 V dc discharge for (a) pure hydrocarbons, (b) pure ammonia and (c) hydrocarbons in ammonia dilution used for nanofibre growth.

3. Results and discussion

Fig. 1 shows OES spectra recorded at a dc bias of 600 V at room temperature. All spectra were averaged over at least five individual measurements to improve the signal-to-noise ratio. Fig. 1a shows emission spectra of three different pure hydrocarbon gases (acetylene, ethylene and methane) taken at 0.7 mbar and normalised to the CH peak at 429 nm, which was the most prominent for all three gases. The C_2 Swan bands at 467 and 516 nm [8] can only be seen for acetylene and ethylene. They are more prominent in acetylene than in ethylene, in accordance with the different appearance energies [9,10]. Fig. 1b shows an emission spectrum taken from a pure ammonia discharge at 1.2 mbar. The most dominant peak is at 335 nm originating from the NH radical [11]. The peak at 389 nm can be assigned to the second positive system of N_2. As in Fig. 1a, H_β and H_γ lines can be seen at 486 and 434 nm, respectively. Fig. 1c shows OES spectra of the three different hydrocarbon gases in ammonia dilution (flow ratio 1:4) recorded at 1.5 mbar and normalized to the NH peak at 335 nm. Compared to the spectra of the pure gases (Fig. 1a,b), for NH_3 diluted CH_4 and C_2H_4 an additional peak at 356 nm appears, which we assign to the second positive system of N_2. The CN peak at 388 nm and the CH peak at 390 nm could not be resolved. However, for methane the centre of the convoluted peak has clearly shifted towards 390 nm. The 389 nm peak of the second positive system of N_2 might also add to the intensity of this convoluted peak. As for Fig. 1a, the C_2 Swan bands are most prominent for diluted acetylene and absent in the CH_4/NH_3 discharge. Elevated temperatures up to 600 °C gave an increase in continuous

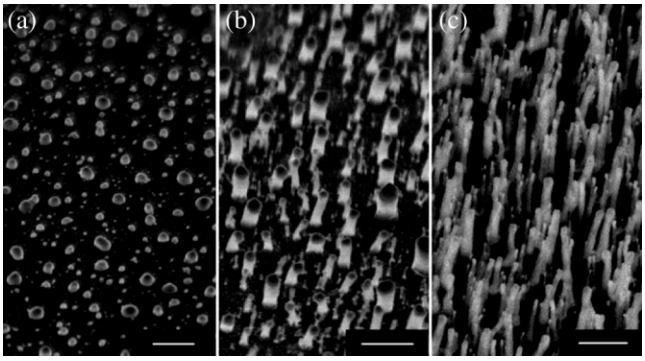

Fig. 2. SEM photographs of a nickel catalyst film after exposure to an ammonia-diluted (a) methane, (b) ethylene and (c) acetylene plasma (flow ratio 1:4) at 450 °C and 1.5 mbar for 10 min (scale bars: (a), (b), (c) 500 nm).

background in accordance with the emitted black body radiation, but did not significantly change position and intensity of the characteristic plasma peaks. Therefore Fig. 1c represents the plasma conditions during nanofibre deposition.

Nanotube growth is a catalytical process, which also works without a plasma. Optical emission spectroscopy solely relates to the plasma atmosphere, whereas no information is obtained about the catalytical surface reactions leading to the actual CNF growth. Nonetheless, a comparison between the species present in the plasma discharge and as-grown CNFs under these conditions is instructive to develop a detailed understanding of the PECVD growth [12].

Fig. 2 shows SEM images of a nickel catalyst film after exposure to ammonia-diluted hydrocarbon plasmas (flow ratio 1:4) at 450 °C and 1.5 mbar for 10 min, characterised by the emission spectra of Fig. 1c. A thin Ni film on a substrate is known to break up into small islands on annealing at elevated temperatures due to surface tension and compressive stress [4]. These islands can act as nucleation sources for subsequent catalytic CNF growth. Despite the plasma atmosphere, diluted methane gave no nanofibre growth (Fig. 2a). At the same conditions, ethylene gave short and stubby vertically aligned CNFs (Fig. 2b), whereas acetylene diluted in ammonia gave an aligned, thick CNF film. At the given conditions with nickel as the catalyst material diluted acetylene clearly shows the highest growth rate. The different growth rates reflect the thermal stability of the corresponding hydrocarbon precursor in the catalytical process, acetylene being the most exothermic. However, the result was compared to thermal growth using the same procedure as for PECVD, except without a dc discharge. At 450 °C, we found the Ni to form islands, but no CNF growth occurred at a pressure of 1.5 mbar even with acetylene as carbon source gas. Therefore, the plasma atmosphere clearly can influence the growth process, which was further studied by measuring the variation of growth rate with temperature in the C_2H_2:NH_3 system.

The role of ammonia in the plasma atmosphere is to etch by-products such as amorphous carbon (a–c). This is not only important for the catalytical growth process itself but also to obtain selective growth without the presence of *a*-C on the substrate surface. Fig. 3a shows vertically aligned CNFs grown from e-beam patterned Ni with a diluted acetylene plasma (C_2H_2:NH_3 ratio 1:4) at 1.5 mbar and 500 °C for 30 min. A Raman map of the sample (Fig. 3c) was obtained by acquiring several thousand individual Raman spectra and plotting

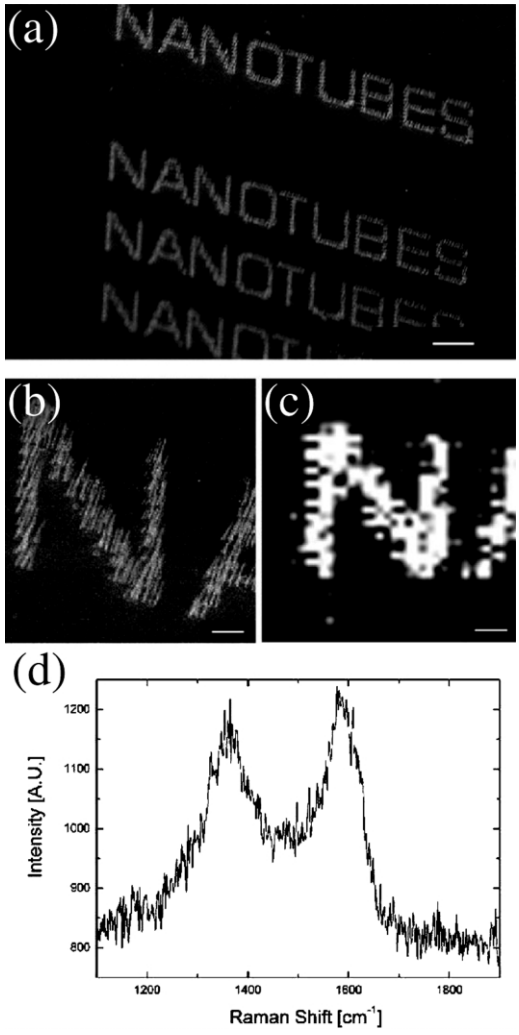

Fig. 3. (a) SEM photograph of vertically aligned CNFs grown from e-beam patterned Ni with a diluted acetylene plasma (C_2H_2:NH_3 ratio 1:4) at 1.5 mbar and 500 °C for 30 min. (b) Close-up of (a) showing the individual aligned CNFs. (c) Corresponding Raman map obtained by acquiring several thousand individual Raman spectra and plotting the integrated, background subtracted intensity signal (between 1070 and 1880 cm^{-1}) over the lateral sample coordinates. (d) Individual Raman spectrum of as-grown CNFs (scale bars: (a) 10 μm and (b), (c) 2 μm).

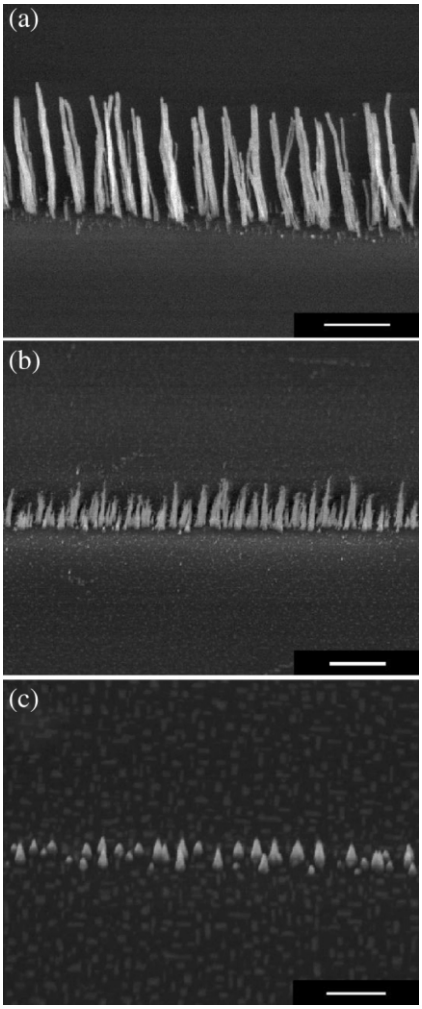

Fig. 4. SEM photographs of vertically aligned CNFs grown with diluted acetylene from e-beam patterned Ni lines at (a) 500 °C, (b) 270 °C and (c) 120 °C. A tilt angle of 40° was used for imaging (scale bars: (a), (b) 1 μm and (c) 500 nm).

the integrated, background subtracted intensity signal (between 1070 and 1880 cm^{-1}) over the lateral sample coordinates. The two main features in the Raman spectra of the as-grown CNFs are the D and G peaks at approximately 1350 and 1600 cm^{-1} (Fig. 3d) [5]. The rather sharp D and G features, together with the evident high frequency shoulder of the G peak, indicate the order and crystallinity of the CNFs [5,13]. Low frequency radial breathing modes are not seen in the CNFs. Raman spectra acquired on the unpatterned substrate areas showed no carbon signal, therefore appearing black on the Raman map. The close resemblance of the Raman map (Fig. 3c) and the corresponding SEM image (Fig. 3b) clearly demonstrates the high selectiveness of the used PECVD method. No carbon, neither amorphous nor graphitic, is deposited outside the patterned region.

Fig. 4 shows single lines of vertically aligned CNFs grown at various temperatures at otherwise unchanged conditions compared to the CNFs shown in Fig. 3a. Nanofibre nucleation can be seen at temperatures as low as 120 °C (Fig. 4c). No CNF growth occurred in plasma conditions without resistive heating. It has to be emphasized that compared to previous literature [14] no separate annealing step at higher temperatures was used to nanostructure the catalyst film into nucleation islands. As comparison, for thermal growth without dc plasma at temperatures below 300 °C neither island formation nor CNF growth was seen. Plasma grown CNFs at lower temperatures appear slightly tapered, with a smaller diameter at the tip than at the bottom. This tapering is due to deposition of amorphous carbon-like material from the plasma along the sidewalls of the growing structure and can be reduced by decreasing the C_2H_2:NH_3 ratio [15].

HREM analysis shows that the degree of crystallinity of the CNFs decreases with decreasing growth temperature (Fig. 5). Vertically aligned CNFs grown at 500 °C with diluted acetylene (Fig. 5a,b) show a characteristic bamboo-like structure [5]. The nanofibres consist of several graphitic shells with a central hollow region, reflecting the crystallinity indicated by the corresponding Raman spectrum in Fig. 3d. CNFs deposited at a lower temperature (Fig. 5c,d) show some well-graphitised areas with their basal planes oriented parallel to the surface of the conical Ni particle at the tip, hence forming a cone-staggered structure. Even lower temperatures give an increasingly amorphous network (Fig. 5e,f). A Ni particle was always found at the tip of the CNFs, suggesting a tip growth mechanism.

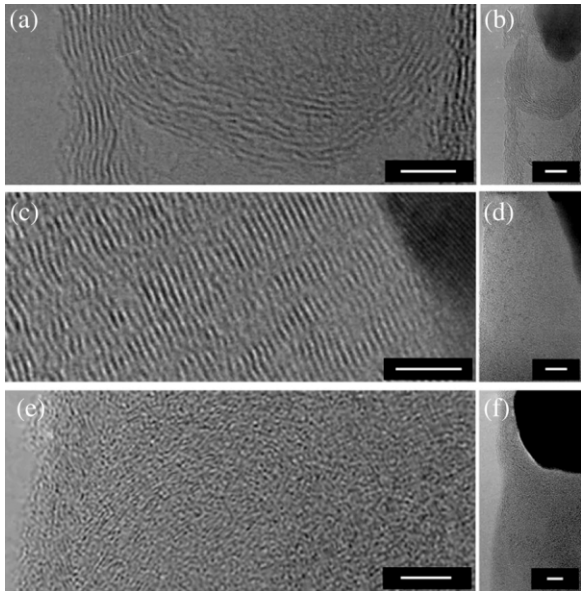

Fig. 5. TEM images of CNFs deposited with diluted acetylene at 500 °C [(a),(b)], 390 °C [(c),(d)] and 270 °C [(e),(f)]. Images (a),(c) and (e) are close-ups of (b),(d) and (f), respectively, (scale bars: 5, 10, 5, 15, 10 and 15 nm, respectively).

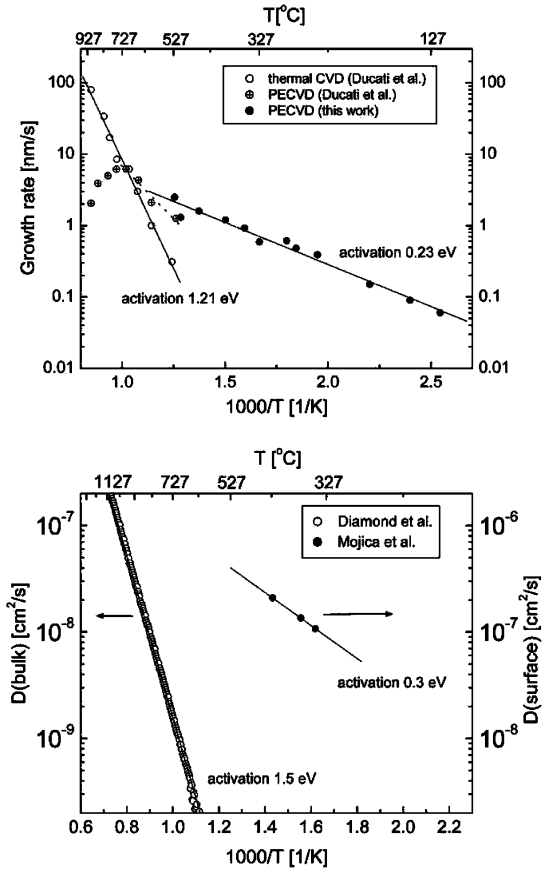

Fig. 6. (a) The CNF growth rate variation with temperature for thermal CVD and PECVD with C_2H_2/NH_3. The data points for thermal CVD and high temperature PECVD are from previous data by Ducati et al. [14]. (b) Temperature dependence of carbon diffusion in nickel from data by Diamond et al. [17] and Mojica et al. [18]. The values for the activation energies were calculated from a linear interpolation of the slopes.

Fig. 6a summarises the variation of growth rate with temperature for the used PECVD process with acetylene as the carbon source. Compared to literature, our measurements cover a wide temperature range from 120 to 900 °C. E-beam patterned single lines of CNFs (Fig. 4) enabled accurate measuring of the fibre length. To eliminate possible variations in catalyst thickness and patterning effects, at each temperature, samples were also grown from a homogeneous Ni film and a 10-μm^2 Ni pattern, and compared to the length of the e-beam patterned CNFs. The catalyst patterning had no effect on the growth rate. The CNF length grew linearly with time, at least up to 30 min, excluding saturation effects on the calculated growth rate.

Most existing models for CVD growth of CNTs and CNFs are based on a mechanism suggested by Baker et al. [16] for the growth of filamentous carbon. The model proposes that the hydrocarbon molecules decompose at the catalyst surface, with the carbon dissolving in the solid metal. The dissolved carbon diffuses through the catalyst particle and precipitates to form a high-aspect ratio carbon structure. In Baker's model for thermal CVD at high temperature, the similarity of the activation energy for filament growth and that for carbon diffusion in the catalyst led to the postulate that the rate determining step is the diffusion of carbon through the particle bulk [16]. Fig. 6a shows the dependence of the growth rate on 1/T for thermal and PECVD, and Fig. 6b shows the variation of diffusion constants with 1/T for bulk and surface diffusion of carbon in nickel. The data points in Fig. 6a for thermal CVD and high-temperature PECVD are taken from previous data [14]. The values for the activation energies were calculated from a linear interpolation of the slopes. The activation energy for thermal CVD (1.21 eV) is similar to that of bulk diffusion of C in nickel (1.5 eV) [17]. The difference may be due to the underestimation of the length of the randomly oriented thermally grown nanotubes at high T. In parallel, the activation energy for PECVD growth (0.23 eV) is similar to that for surface diffusion of C on polycrystalline Ni (0.3 eV) [18]. Therefore, we suggest that the diffusion of carbon on the catalyst surface is the rate-determining step at low temperatures. The diffusion of carbon is mainly driven by a concentration gradient, rather than a temperature gradient as originally suggested by Baker et al. [16,19].

The effect of the plasma can be to increase the dissociation of the precursor gases, as well as to cause a local surface heating that enables an efficient adsorption and diffusion of the carbon atoms. A key role of the plasma is to nanostructure the initial Ni film and etch any *a*-C, which may cover the catalyst particle during growth, and is thereby providing a steady supply of carbon at the top surface of the Ni particle. At low temperatures, the solubility of C in Ni is low, so the amount of carbon diffusing through the particle is limited. However, carbon atoms adsorbed at the top surface of the Ni particle can diffuse along the surface, where their motion is much faster. Carbon then segregates at the bottom of the particle, forming graphitic planes. This process allows CNF growth at such low temperatures.

4. Conclusions

Investigating the effects of the different carbon source gases on the PECVD growth of CNFs, we found that acetylene offers the highest growth rate in conjunction with ammonia as an etchant and nickel as catalyst material. Focussing on acetylene, we demonstrated the controlled, selective synthesis of vertically aligned carbon nanofibres on prepatterned substrates at temperatures as low as 120 °C and presented a growth mechanism based on a surface diffusion process. The result allows more cost-effective CNF production, direct growth of nanofibres onto low-temperature substrates

like plastics [20], and could facilitate CNF integration into sensitive nanoelectronic devices.

Acknowledgments

This work was supported by the EU project CARDECOM GRD1-2001-41830. ACF acknowledges funding from The Royal Society.

References

[1] T.W. Ebbesen, P.M. Ajayan, Nature 358 (1992) 220.
[2] A. Thess, R. Lee, P. Nikolaev, H. Dai, P. Petit, J. Robert, et al., Science 273 (1996) 483.
[3] Z.F. Ren, Z.P. Huang, J.W. Xu, J.H. Wang, P. Bush, M.P. Siegal, et al., Science 282 (1998) 1105.
[4] V.I. Merkulov, D.H. Lowndes, Y.Y. Wei, G. Eres, E. Voelkl, Appl. Phys. Lett. 76 (2000) 3555.
[5] M. Chhowalla, K.B.K. Teo, C. Ducati, N.L. Rupesinghe, G.A.J. Amaratunga, A.C. Ferrari, et al., J. Appl. Phys. 90 (2001) 5308.
[6] B.O. Boskovic, V. Stolojan, R.U.A. Khan, S. Haq, S.R.P. Silva, Nat. Mater. 1 (2002) 165.
[7] S. Hofmann, C. Ducati, J. Robertson, B. Kleinsorge, Appl. Phys. Lett. 83 (2003) 135.
[8] R.W.B. Pearse, A.G. Gaydon, The Idendification of Molecular Spectra, Chapman and Hall, London, 1963.
[9] I.H. Suzuki, K. Maeda, Mass Sp. 25 (1977) 223.
[10] K. Maeda, I.H. Suzuki, Y. Koyama, Int. J. Mass. Spectrom. Ion Processes 14 (1974) 273.
[11] H. Sekiya, N. Nishiyama, M. Tsuji, Y. Nishimura, J. Chem. Phys. 86 (1987) 163.
[12] D. Hash, D. Bose, T.R. Govindan, M. Meyyappan, J. Appl. Phys. 93 (2003) 6284.
[13] A.C. Ferrari, J. Robertson, Phys. Rev. B 61 (2000) 14095.
[14] C. Ducati, I. Alexandrou, M. Chhowalla, G.A.J. Amaratunga, J. Robertson, J. Appl. Phys. 92 (2002) 3299.
[15] V.I. Merkulov, M.A. Guillorn, D.H. Lowndes, M.L. Simpson, E. Voelkl, Appl. Phys. Lett. 79 (2001) 1178.
[16] R.T.L. Baker, M.A. Barber, in: P.L. Walker, P.A. Thrower (Eds.), Chemical Physics and Carbon, Dekker, New York, 1978, p. 83.
[17] S. Diamond, C. Wert, Trans. AIME 239 (1967) 705.
[18] J.F. Mojica, L.L. Levenson, Surf. Sci. 59 (1976) 447.
[19] A. Oberlin, M. Endo, T. Koyama, J. Cryst Growth 32 (1976) 335.
[20] S. Hofmann, C. Ducati, B. Kleinsorge, J. Robertson, Appl. Phys. Lett. 83 (2003) 4661.